Applied Microbiology and Biotechnology (2021) 105:4675–4691
https://doi.org/10.1007/s00253-021-11370-3

APPLIED GENETICS AND MOLECULAR BIOTECHNOLOGY

G protein γ subunit modulates expression of plant-biomass-degrading enzyme genes and mycelial-development-related genes in *Penicillium oxalicum*

Xiao-Ming Pang[1] · Di Tian[1] · Ting Zhang[1] · Lu-Sheng Liao[1] · Cheng-Xi Li[1] · Xue-Mei Luo[1] · Jia-Xun Feng[1] · Shuai Zhao[1]

Received: 1 March 2021 / Revised: 5 May 2021 / Accepted: 26 May 2021 / Published online: 2 June 2021

Abstract

Heterotrimeric-G-protein-mediated signaling pathways modulate the expression of the essential genes in many fundamental cellular processes in fungi at the transcription level. However, these processes remain unclear in *Penicillium oxalicum*. In this study, we generated knockout and knockout-complemented strains of *gng-1* (*POX07071*) encoding the Gγ protein and found that GNG-1 modulated the expression of genes encoding plant-biomass-degrading enzymes (PBDEs) and sporulation-related activators. Interestingly, GNG-1 affected expression of the *cxrB* that encodes a known transcription factor required for the expression of major cellulase and xylanase genes. Constitutive overexpression of *cxrB* in Δ*gng-1* circumvented the dependence of PBDE production on GNG-1. Further evidence indicated that CxrB indirectly regulated the transcription levels of key amylase genes by controlling the expression of the regulatory gene *amyR*. These data extended the diversity of Gγ protein functions and provided new insight into the signal transduction and regulation of PBDE gene expression in filamentous fungi.

Key points

- *GNG-1 modulates the expression of PBDE genes and sporulation-related genes.*
- *GNG-1 controls expression of the key regulatory gene cxrB.*
- *Overexpression of cxrB circumvents dependence of PBDE production on GNG-1.*

Keywords G protein gamma subunit · GNG-1 · Plant-biomass-degrading enzyme · CxrB · *Penicillium oxalicum*

Introduction

Filamentous fungi are widely distributed in soil (Powers-Fletcher et al. 2016; Zhang et al. 2014) and have a strong capacity to degrade macropolymers such as cellulose, xylan, and starch in plant biomass. This ability is dependent upon the secretion of carbohydrate-active enzymes (CAZymes), which are essential for the carbon cycle and climatic changes (Gougoulias et al. 2014). The secretion of CAZymes by filamentous fungi is strictly controlled, specifically at the transcription level (Benocci et al. 2017). With decades of effort, several transcription factors (TFs) involved in the regulation of PBDE (plant-biomass-degrading enzyme) gene expression in fungi have been identified, including AmyR and CxrB (Li et al. 2017; Schmoll 2018). CxrB positively regulates the expression of cellulase and xylanase genes in *Penicillium oxalicum* (Schmoll et al. 2009; Yan et al. 2017), and AmyR activates the expression of major amylase genes and represses the transcription of cellulase genes in this fungus (Li et al. 2015).

G-protein-mediated signaling pathways modulate multiple biological processes, including growth,

✉ Shuai Zhao
shuaizhao0227@gxu.edu.cn

[1] State Key Laboratory for Conservation and Utilization of Subtropical Agro-bioresources, Guangxi Research Center for Microbial and Enzyme Engineering Technology, College of Life Science and Technology, Guangxi University, 100 Daxue Road, Nanning, Guangxi 530004, People's Republic of China

development, and virulence (Chakravorty and Assmann 2018). The conventional G protein consists of subunits Gα, Gβ, and Gγ, which form the heterotrimeric complex Gαβγ in the inactive state. In most filamentous fungi, the Gα proteins are classified into three groups. Groups I and III Gα proteins contribute to vegetative growth, development, and pathogenesis, whereas Group II proteins play minor roles (Li et al. 2007; Liu et al. 2018). Under environmental stimulation, G-protein-coupled receptors are activated, and then bind and activate G proteins, leading to the separation of Gα from the heterodimer Gβγ and GTP-GDP exchange on Gα. The separated Gα and heterodimer Gβγ then drive specific downstream effector proteins, mainly including adenylate cyclase/cAMP, mitogen-activated protein (MAP) kinases, and phospholipase C (Chakravorty and Assmann 2018; Li et al. 2007).

Accumulating evidence indicates that the Gα-protein-mediated signaling pathway is linked to the regulation of cellulase and amylase genes in filamentous fungi. In *Trichoderma reesei*, the Gα proteins GNA1 and GNA3 play important roles in cellulase gene expression in the presence of cellulose, and their expression is light-dependent (Schmoll et al. 2009; Seibel et al. 2009). In the chestnut blight fungus *Cryphonectria parasitica*, the Gα protein CPG-1 is required for cellobiohydrolase I gene (*cbh1*) expression (Wang and Nuss 1995). In *P. oxalicum*, the deletion of the gene *PGA3* encoding Gα protein PGA3 reduces amylase production and the transcription of the key amylase gene *Amy15A*, whereas it causes no significant change in cellulase production, although the expression of cellobiohydrolase gene *cbh1* is increased in mutant Δ*pga3* (Hu et al. 2013). These data imply that the function of Gα is species-independent. Furthermore, the Gα proteins of *T. reesei* and *P. oxalicum* are involved in the expression of cellulase and amylase genes by controlling intracellular cAMP levels (Schmoll et al. 2009; Hu et al. 2013; Schuster et al. 2012).

In contrast to the Gα proteins, few studies have reported the roles of the Gβ and Gγ proteins in the production of PBDEs in filamentous fungi. Tisch and collaborators (Tisch et al. 2011) found that the individual loss of the Gβ or Gγ proteins GNB1 or GNP1, respectively, increased cellulase production, and conversely reduced the transcription of major cellulase genes, including *cbh1*, in *T. reesei*, independently of the light status. However, how Gβγ modulates the expression of PBDE genes via TFs and whether its functions are species-specific require further research.

In this study, we showed that the Gγ subunit GNG-1 (POX07071) was required for the expression of PBDE (cellulase, xylanase, and amylase) genes and mycelial-development-related genes, which needed the contribution of an important TF CxrB in *P. oxalicum*.

Materials and methods

Fungal strains and their culture conditions

The *P. oxalicum* parental strain Δ*ku70*, deposited in the China General Microbiological Culture Collection (CGMCC) under accession number 3.15650, was derived from wild-type strain HP7-1 (CGMCC no. 10781) by the deletion of the *ku70* gene, which is involved in the classic non-homologous end-joining pathway (Zhao et al. 2016). The other *P. oxalicum* mutants listed in Table 1 were generated in the parental strain Δ*ku70* with a homologous double-crossover methodology. The chosen transformants were confirmed by PCR amplification with specific primers (Supplementary Table S1 and Fig. S1A) and Southern hybridization with specific probes (Supplementary Table S1 and Fig. S1B). All *P. oxalicum* strains were cultured on potato-dextrose agar (PDA) plates at 4°C for temporary storage. Fungal spores were collected from PDA plates precultured for 6 days at 28°C with 0.1% Tween 80, and were adjusted to a concentration of 1×10^8 per mL, before their use in fungal reproduction.

The *P. oxalicum* strains were cultured according to the method described by Zhao and collaborators (Zhao et al. 2016) for the measurement of cellulase and xylanase production, as well as amylase production, except that the carbon source (Avicel) was replaced with soluble corn starch (SCS) (Sigma-Aldrich, St. Louis, MO, USA).

For RNA-Seq and RT–qPCR analyses, the *P. oxalicum* strains were cultured for 4–48 h as described above. The mycelia used for total RNA extraction were collected every 12 h.

The *P. oxalicum* strains were cultured on MMM plates containing glucose, Avicel, or soluble corn starch (Sigma-Aldrich, St. Louis, MO, USA) or on PDA plates at 28°C, for 20 h for microscopic analyses and for 3 days for colony analyses.

Extraction of fungal DNA and RNA

Total DNA and RNA were extracted from the *P. oxalicum* strains as described by Zhao et al. (2016). The quality and quantity of the extracted DNA and RNA were evaluated with electrophoresis on 1.0% agarose gel and a NanoDrop 2000 spectrophotometer (Thermo Fisher Scientific, Waltham, MA, USA).

Construction of deletion mutants and complementation strains

The methods used to construct the deletion mutants and their corresponding complementation strains in the *P. oxalicum* parental strain Δ*ku70* were reported by Yan et al. (2017).

Table 1 *Penicillium oxalicum* strains used in this work

Strains	Genotypes	References
Δ*ku70*	*ku70*$^{-}$; *hph*$^{R+}$	(Zhao et al. 2016)
Δ*gng-1*	*ku70*$^{-}$; *gng-1*$^{-}$; *hph*$^{R+}$; *G418*$^{R+}$	This study
Δ*gng-1::gng-1*	*gng-1*$^{+}$; *hph*$^{R+}$; *G418*$^{R+}$; *Ble*$^{R+}$	This study
Δc*xrB*	k*u70*$^{-}$; c*xrB*$^{-}$; *hph*$^{R+}$; *G418*$^{R+}$	(Yan et al. 2017)
ΔcxrB::cxrB	c*xrB*$^{+}$; ku70^{-}; *hph*$^{R+}$; *G418*$^{R+}$; *Ble*$^{R+}$	(Yan et al. 2017)
Δgng-*1*::c*xrB*	gng-*1*$^{-}$; ku70^{-}; c*xrB* overexpression; *hph*$^{R+}$; *G418*$^{R+}$; *Ble*$^{R+}$	This study
Δgng-*1*::gng-$1_{1\text{-}85}$	ku70^{-}; gng-1^{-}; gng-$1_{1\text{-}85}$$^{+}$; *hph*$^{R+}$; *G418*$^{R+}$; *Ble*$^{R+}$	This study

Hph^{R+} hygromycin B-resistant gene; *G418*$^{R+}$ geneticin-resistant gene; *Ble*$^{R+}$ bleomycin-resistant gene

Construction of overexpression strains

The overexpression strains of *P. oxalicum* were constructed as described for the complementation strains, except that the encoding sequence of the complementation gene was replaced by the overexpressed gene with the native promoter or the constitutive promoter p*TEF1*.

RNA-Seq and data analysis

RNA sequencing (RNA-Seq) of the *P. oxalicum* strains was as previously reported (Li et al. 2020). Total RNAs were extracted from each *P. oxalicum* strain cultivated on Avicel for 24 h after a transfer. Three biological replicates of each sample were sequenced and further analyzed. The appropriate RNA was used to construct a library of single-stranded circular DNAs, which were then sequenced on the BGI-SEQ-500 platform at BGI, Shenzhen, China. The raw reads generated were filtered with SOAPnuke v1.5.2 (Chen et al. 2018) to generate clean reads. The clean reads were mapped onto the genome of *P. oxalicum* strain HP7-1 and annotated with Hierarchical Indexing for Spliced Alignment of Transcripts v2.0.4 (Kim et al. 2015) and Bowtie2 v2.2.5 (Langmead and Salzberg 2012). The transcript levels of the genes were represented as fragments per kilobase of exon per million mapped reads (FPKM) values, which were obtained with RSEM v1.2.12 (Li and Dewey 2011). The differentially expressed genes (DEGs) were detected with DESeq tool (Love et al. 2014), with cutoff values of $q \leq 0.05$ and $|\log2(\text{fold change})| \geq 1$.

RT-qPCR analysis

RT-qPCR was used to compare the gene transcription levels in different fungal strains based on a previously described method (Yan et al. 2017). The specific primers corresponding to each target gene were shown in Supplementary Table S1. The relative expression of each target gene was calculated with the $2^{-\Delta\Delta CT}$ method (Livak and Schmittgen 2001). The actin-encoding gene *POX09428* was used as the internal control gene, and the expression of all the target genes was normalized to the expression level in the parental strain Δ*ku70*. Three independent biological replicates of each RT–qPCR experiment were performed.

Measurement of PBDE production

The production of PBDEs, including cellulases, xylanases, raw-cassava-starch-degrading enzymes (RSDEs), and soluble-starch-degrading enzymes (SSDEs), were measured with the methods reported by Yan et al. (2017) and Wang et al. (2018). The enzymatic activity units (U) for filter paper cellulase (FPase), carboxymethylcellulase (CMCase), xylanase, SSDEs and RSDEs were defined as the amount of enzyme that produced 1 μmoL of reducing sugar per minute from the appropriate substrate, whereas 1 unit of *p*-nitrophenyl-β-cellobiosidase (pNPCase) or *p*-nitrophenyl-β-glucopyranosidase (pNPGase) was the amount of enzyme that produced 1 μmoL of *p*-nitrophenol per minute from the appropriate substrate. Each experiment was performed independently at least three times.

Southern hybridization analysis

The deletion mutant of *P. oxalicum* was analyzed with Southern hybridization to confirm the insertion of the knockout DNA cassette at a single locus in the chromosome. Southern hybridization was performed as previously described (Zhao et al. 2016).

Measurement of *P. oxalicum* biomass

The accumulated mycelial weights of *P. oxalicum* cultured in MMM containing either glucose or SCS were quantified after the mycelia were dried at 50°C. When the *P. oxalicum* strains were cultured in MMM containing Avicel as the sole carbon source, the intracellular proteins were extracted from the collected mycelia, and represented the true mycelial accumulation. The intracellular proteins were extracted with protein extraction buffer (g/L: NaCl 8.5, Na_2HPO_4 2.2, NaH_2PO_4 0.2, phenylmethylsulfonyl fluoride 0.87,

ethylenediaminetetraacetic acid 1.86, pH 7.4] based on the method of Li and collaborators (Li et al. 2020). The mycelia were collected from the *P. oxalicum* cultures every 12 h until 72 h. All experiments were performed independently in triplicate.

Determination of asexual spore numbers

Fresh spores (1×10^5) from the *P. oxalicum* strains were spread on plates containing Avicel, SCS, or glucose, or PDA plates. The inoculated Avicel- and SCS-containing plates were incubated at 28°C for 10 days, whereas the inoculated glucose- and PDA-containing plates were incubated for 15 and 3 days, respectively. More than 10 samples (1 cm^2) of each strain were taken with a hole puncher. The asexual spores were washed with 0.1% Tween 80 and counted with a hemocytometer after the appropriate dilution. Triplicate biological repetitions of each experiment were performed.

In vitro electrophoretic mobility shift assay (EMSA) and competitive EMSA

In vitro EMSA and competitive EMSA were performed as described by Yan et al. (2017). The tested genes were amplified by PCR with specific primers (Supplementary Table S1).

Bioinformatic analysis

Homologous protein sequences of GNG-1 were screened on the National Center for Biotechnology Information BlastP website (https://blast.ncbi.nlm.nih.gov/Blast.cgi) and then downloaded for further analysis. A phylogenetic tree was constructed with MEGA version X (Kumar et al. 2018) with the neighbor-joining method and a Poisson correction model. Bootstrap values were calculated from 1000 replicates. A sequence alignment was constructed in MUSCLE online with Clustal W (https://www.ebi.ac.uk/Tools/msa/muscle/).

Investigation of colony phenotypes and hyphae

P. oxalicum colonies on solid plates were directly photographed with a Canon EOS 6D camera (Canon Inc., Tokyo, Japan). The hyphae of *P. oxalicum* were examined with light microscopy (Olympus DP480; Olympus, Tokyo, Japan). The harvested hyphae were transferred onto microscope slides with phosphate-buffered saline. The photomicrographs were analyzed with cellSens Dimension digital imaging software (Olympus).

Subcellular localization of protein CxrB

GFP was used as the reporter protein to visualize the subcellular localization of CxrB in *P. oxalicum* hyphae. The expression of *gfp*-labeled *cxrB* was enhanced by using the inducible promoter pPoxEGCel5B (Wang et al. 2018).

Statistical analysis

All experimental data were analyzed statistically with Student's *t* test in Microsoft Excel (Office 2016) (Microsoft, Redmond, WA, USA).

Accession number

Sequence of GNG-1 was uploaded in GenBank with accession number MT993961. Transcriptomic data of *P. oxalicum* strains have been deposited in the Sequence Read Archive database (Accession No. GSE154704)

Results

Sequence analysis of Gγ protein GNG-1 in *P. oxalicum*

When we screened the annotated proteins encoded in the *P. oxalicum* strain HP7-1 genome (Zhao et al. 2016), *POX07071* was predicted to encode the G protein subunit Gγ. The protein POX07071 contained 90 amino acids, a Gγ-like domain (GGL; amino acids 20–90; *E*-value = 2.39e−14) (Fig. 1A), and the CCAAX (cysteine, cysteine, aliphatic, aliphatic, X [any residue]) box CCTVM at the C-terminus (Fig. 1B). A BlastP alignment indicated that POX07071 shared 100%, 95.6%, 67.7%, 65.6%, and 30.95% identity with Gγ proteins in *P. oxalicum* strain 114-2, *Aspergillus clavatus* NRRL 1, *T. reesei* QM6a, *Neurospora crassa* OR74A, and *Saccharomyces cerevisiae* S288C, respectively.

A neighbor-joining phylogenetic analysis showed that POX07071 had close evolutionary relationships with homologues in some *Aspergillus*, but more distant relationships with those of *T. reesei* and *S. cerevisiae* (Fig. 1C). To facilitate further study, POX07071 was redesignated GNG-1.

GNG-1 modulates the production of PBDE in *P. oxalicum*

To investigate the effects of GNG-1 on PBDE (cellulase, xylanase, and amylase) production in *P. oxalicum*, the deletion mutant Δ*gng-1* was constructed (Supplementary Fig. S1A), and confirmed with PCR and Southern hybridization analyses (Supplementary Fig. S1A and B). After preculture in glucose medium for 24 h, the mutant Δ*gng-1* and the parental strain Δ*ku70* were cultured for 2–4 days in MMM containing Avicel (Sigma-Aldrich) as the sole carbon source, and their cellulase and xylanase production were determined. The production of cellulases (FPase, CMCase, and pNPCase) by the mutant Δ*gng-1* was 50.8–96.1% lower than that of Δ*ku70* and

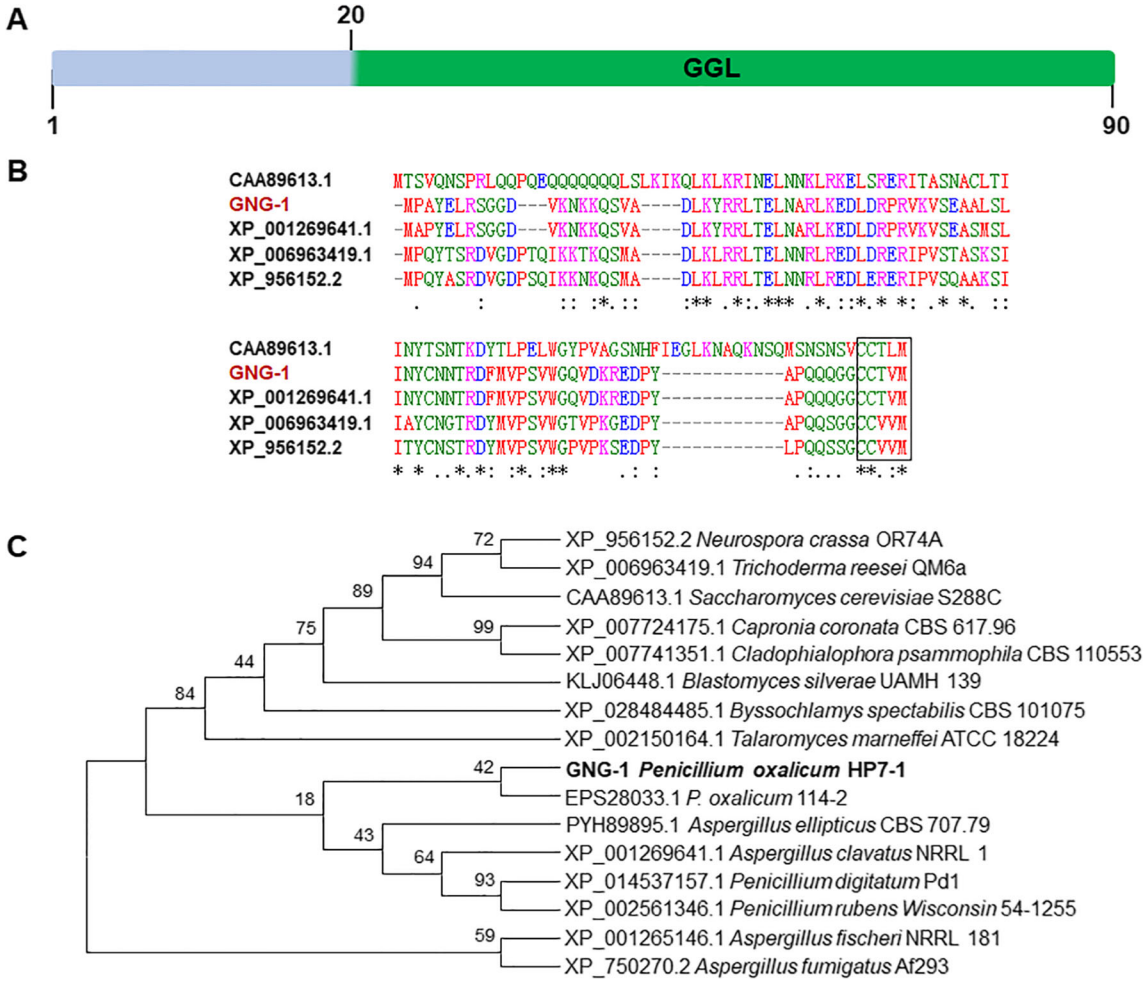

Fig. 1 Sequence analysis of G protein gamma subunit GNG-1 (POX07071) of *P. oxalicum*. (**A**) Conserved domain of GNG-1: GGL, G-protein gamma-like domain. (**B**) Multiple alignment of GNG-1 and its orthologues. CAA89613.1: Ste18p from *Saccharomyces cerevisiae* S288C; XP_00126964.1: Ste18/GpgA from *Aspergillus clavatus* NRRL 1; XP006963419.1: Gpg1 from *Trichoderma reesei* QM6a; XP_956152.2: Gpg from *Neurospora crassa* OR74A. Black frame marks the conserved CCAAX box (cysteine, cysteine, aliphatic, aliphatic, X [any residue]). Red residues indicate small amino acids (small + hydrophobic, including aromatic tyrosine). Blue residues indicate acidic amino acids. Magenta residues indicate basic amino acid histidine. Green residues indicate hydroxyl + sulfhydryl + amine + glycine. "*" indicates that the amino acids are identical in all the aligned sequences. ":" indicates conserved amino acids with very similar properties. "." indicates conserved amino acids with weakly similar properties. (C) Phylogenetic tree constructed with MEGA version X software. The neighbor-joining method was used with a Poisson model. Bootstrap values were calculated from 1000 replicates

the production of xylanase was 40.9–80.6% lower than that of Δ*ku70* (all $P < 0.01$; Fig. 2A–C and E). Notably, the deletion of *gng-1* caused a 29-fold increase in pNPGase production after culture for 2 days, and a 10.7% increase after 4 days ($P < 0.05$; Fig. 2D).

After preculture in glucose medium for 24 h, the deletion mutant Δ*gng-1* and the parental strain Δ*ku70* were cultured for 2–4 days in MMM containing SCS at 28 °C with shaking at 180 rpm, and their production of SSDEs and RSDEs was measured. SSDE and RSDE production in Δ*gng-1* was 49.3–77.8% lower than that in the parental strain Δ*ku70* (all $P < 0.01$; Fig. 2F and G).

To confirm that the change in PBDE production resulted from the deletion of *gng-1* in *P. oxalicum*, the complementation experiment was performed. The complementation strain Δ*gng-1*::*gng-1* was constructed, with *gng-1* expressed under the native promoter inserted into a protease gene (*POX05007*) locus (Supplementary Fig. S1C). The complementation strain Δ*gng-1*::*gng-1* restored PBDE production to the levels observed in Δ*ku70* ($P > 0.05$; Fig. 2). These data demonstrated that the changes in PBDE production in Δ*gng-1* resulted from the deletion of *gng-1*.

The CCAAX motif at the C-terminus of Gγ can be modified with a farnesyl or geranylgeranyl moiety, which is required for the membrane association of the heterodimer

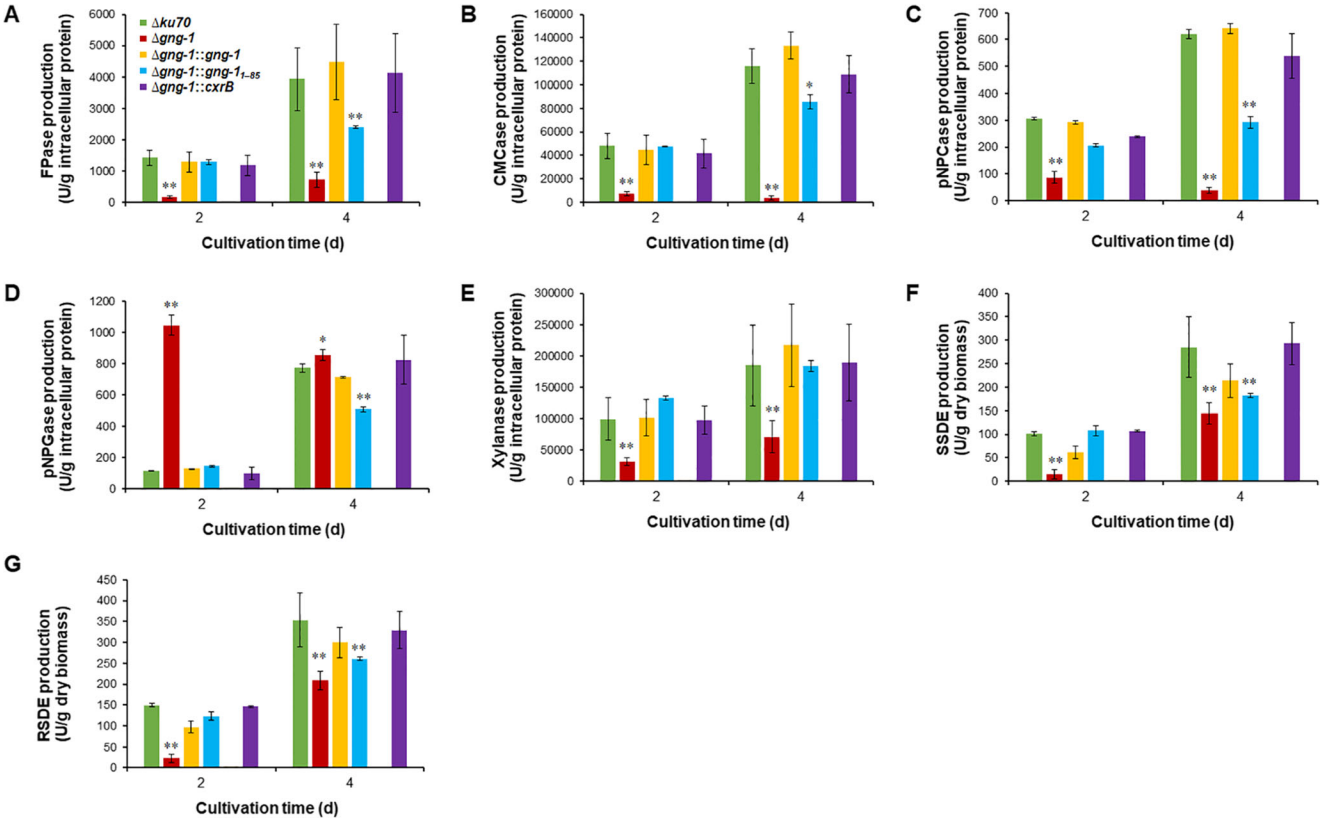

Fig. 2 PBDE production in *P. oxalicum* strains. Mutant strain Δ*gng-1*, parental strain Δ*ku70*, complementation strain Δ*gng-1*::*gng-1*, and truncated complementation strain Δ*gng-1*::*gng-1*$_{1–85}$ were cultured in MMM containing Avicel for cellulase and xylanase production or soluble corn starch for amylase production for 2–4 days at 28°C with shaking at 180 rpm after their transfer from glucose. (**A**) FPase; (**B**) CMCase; (**C**) pNPCase; (**D**) pNPGase; (**E**) xylanase; (**F**) SSDE; (**G**) RSDE. FPase, filter paper cellulase; CMCase, carboxymethylcellulase; pNPCase, *p*-nitrophenyl-β-cellobiosidase; pNPGase, *p*-nitrophenyl-β-glucopyranosidase; MMM: modified minimal medium; SSDE: soluble-starch-degrading enzyme; RSDE: raw-cassava-starch-degrading enzyme. Data points represent means ± standard deviations. $^{**}P \leq 0.01$ on Student's *t*-test, indicating significant differences between each mutant or complementation strain and the parental strain Δ*ku70*

Gβγ (Alvaro and Thorner 2016). To investigate effects of the CCAAX motif on PBDE production, we constructed the strain Δ*gng-1*::*gng-1*$_{1–85}$ in which the introduced *gng-1* lacked the sequence encoding the CCAAX motif (Supplementary Fig. S1D). When cultured for 4 days in MMM containing Avicel as the sole carbon source, Δ*gng-1*::*gng-1*$_{1–85}$ partly lost the ability to produce cellulase, producing only 60.8%–73.7% of cellulase produced by Δ*ku70* ($P < 0.01$; Fig. 2A–D). Surprisingly, the production of xylanase by Δ*gng-1*::*gng-1*$_{1–85}$ was normal (Fig. 2E). As we expected, SSDE and RSDE production by Δ*gng-1*::*gng-1*$_{1–85}$ decreased by 35.8% and 32.4% in comparison with those of Δ*ku70*, respectively ($P < 0.01$; Fig. 2F and G). These results indicated that the CCAAX motif modified with a farnesyl or geranylgeranyl moiety was required for cellulase and amylase production.

GNG-1 positively affects mycelial growth and conidiation in *P. oxalicum*

To determine the effects of GNG-1 on fungal mycelial growth, solid MMM plates containing glucose, Avicel, or SCS or PDA plates were inoculated with the *P. oxalicum* mutant Δ*gng-1*, the parental strain Δ*ku70*, or the complementation strain Δ*gng-1*::*gng-1* and Δ*gng-1*::*gng-1*$_{1–85}$, and incubated at 28 °C for 3 days. The Δ*gng-1* colonies showed irregular edge on PDA, glucose and SCS, while colonies of the Δ*ku70*, Δ*gng-1*::*gng-1*, and Δ*gng-1*::*gng-1*$_{1–85}$ exhibited regular edge. The Δ*gng-1* colony on SCS was smaller than those of the others. The color of the Δ*gng-1* on all tested plates showed some degree of alteration compared with those of the Δ*ku70* and Δ*gng-1*::*gng-1*. The Δ*gng-1*::*gng-1* colonies were slightly larger than those of Δ*ku70*, whereas their color was similar (Fig. 3).

After the four *P. oxalicum* strains were cultured on solid medium plates for 20 h, the hyphae were collected for

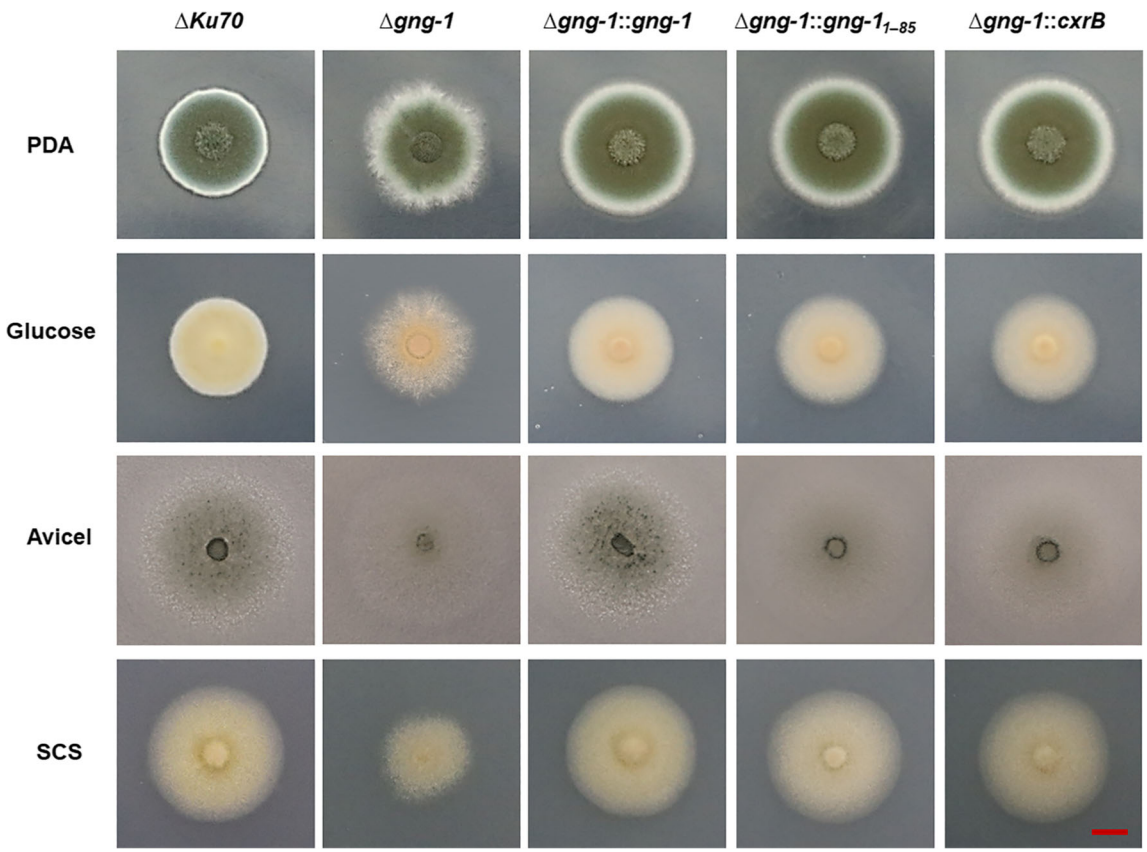

Fig. 3 Phenotypic analysis of *P. oxalicum* strains. (**A**) Colony characteristics. *P. oxalicum* mutant strain Δ*gng-1*, parental strain Δ*ku70*, complementation strain Δ*gng-1*::*gng-1*, and truncated complementation strain Δ*gng-1*::*gng-1*$_{1–85}$ were grown directly on solid plates containing MMM with different carbon sources for 3 days at 28°C. Scale bar = 0.9 cm. MMM: modified minimal medium; PDA: potato dextrose agar; SCS: soluble corn starch

microscopic evaluation. The hyphae of Δ*gng-1* and Δ*gng-1*::*gng-1*$_{1–85}$ produced conidiophores, whereas those of Δ*ku70* and Δ*gng-1*::*gng-1* did not (Fig. 4A and B). However, at 48 h, the hyphae of all the *P. oxalicum* strains produced conidiophores (Supplementary Fig. S2). It is noteworthy that the expression of *gng-1*$_{1–85}$ in mutant Δ*gng-1* did not restore conidiospore production to the level in Δ*ku70*, suggesting that the deleted CCAAX motif controlled the time at which hyphae produce conidiospores. In addition to this difference in conidiospore production, the branches of the Δ*gng-1* hyphae were less abundant than those of Δ*ku70*, Δ*gng-1*::*gng-1*, and Δ*gng-1*::*gng-1*$_{1–85}$ during the whole culture period. However, the hyphal branches of Δ*ku70*, Δ*gng-1*::*gng-1*, and Δ*gng-1*::*gng-1*$_{1–85}$ were similar (Fig. 4; Supplementary Fig. S2).

The asexual spores produced by the mutant Δ*gng-1* were counted grown on PDA plates and plates containing Avicel, glucose, or SCS. Both Δ*ku70* and Δ*gng-1*::*gng-1* were used as controls. The number of spores produced by Δ*gng-1* was only 33.3–50.1% of the control values ($P < 0.01$), although there was no significant difference between Δ*ku70* and Δ*gng-1*::*gng-1* (Fig. 4C), suggesting that GNG-1 is positively involved in spore production in *P. oxalicum*. The number of spores produced by Δ*gng-1*::*gng-1*$_{1–85}$ was also lower than the number produced by Δ*ku70*, indicating that the CCAAX motif of GNG-1 was involved in spore production by *P. oxalicum*.

Liquid MMM containing glucose, Avicel, or SCS was inoculated with strain Δ*gng-1* or Δ*ku70* and incubated at 28 °C for 72 h to construct their growth curves. The biomass accumulation in the Δ*gng-1* culture in MMM containing either glucose or SCS as the sole carbon source decreased markedly by 35.1–50.2% or 11.3–57.2%, respectively, of the control (Δ*ku70*) value (both $P < 0.05$) after 12 h in culture (Fig. 5A and B). However, at 12 h, the mutants Δ*gng-1* and Δ*ku70* showed similar biomass accumulation in glucose (Fig. 5A). However, the biomass accumulated by Δ*gng-1* in SCS medium was reduced to 49.9% of the control value (Fig. 5B). By contrast, in medium containing Avicel, the amount of intracellular proteins in Δ*gng-1* was less than that in Δ*ku70* at 12 h but similar to that in Δ*ku70* at 24–48 h, although this was followed by a 22.4–30.3% reduction relative to that in the Δ*ku70* ($P < 0.05$; Fig. 5C). Therefore, GNG-1 was involved in the growth of *P. oxalicum*, independently of the carbon source.

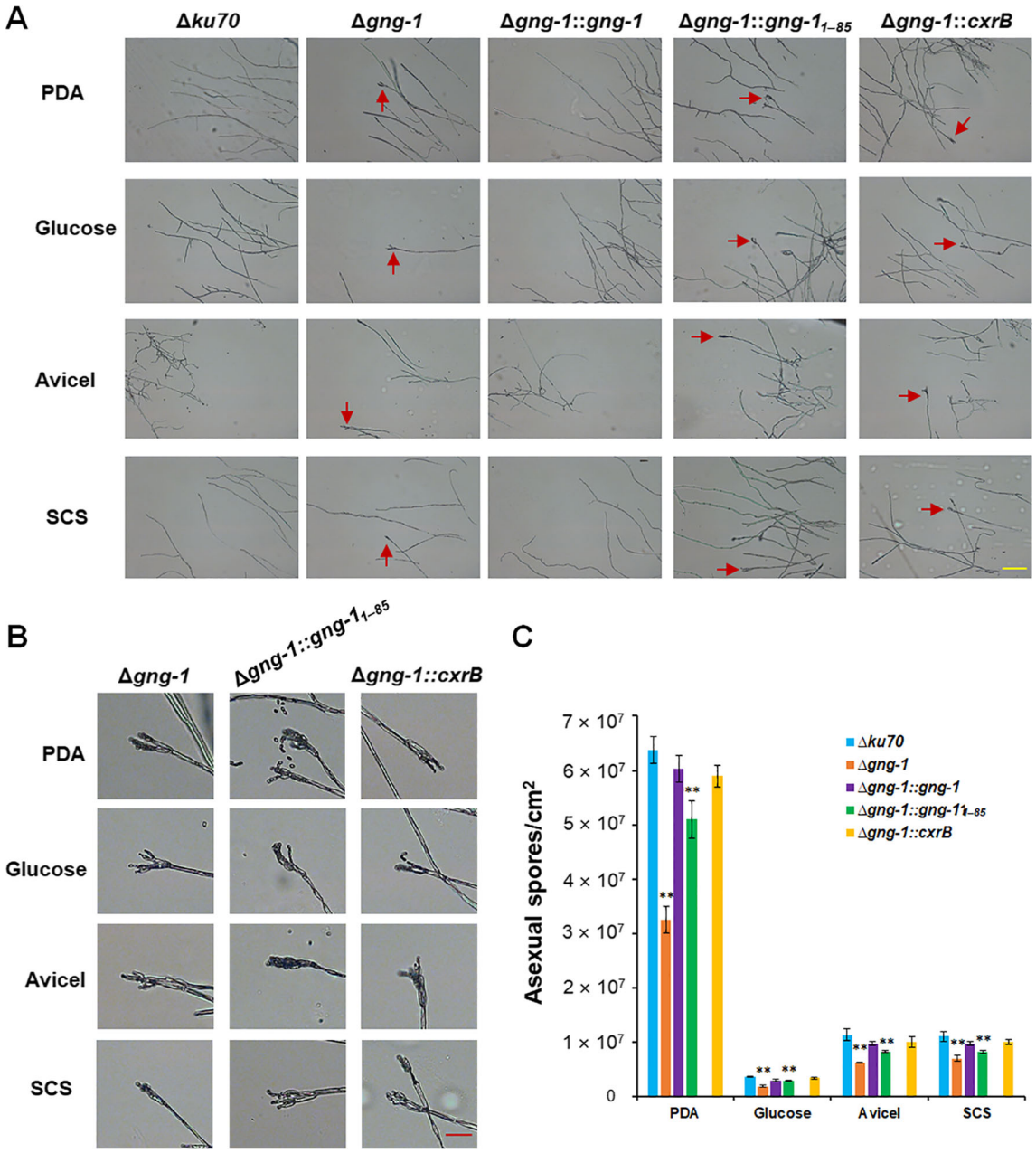

Fig. 4 Microscopic investigation of hyphae and asexual spores. (**A**) *P. oxalicum* hyphae. Mutant strain Δ*gng-1*, parental strain Δ*ku70*, complementation strain Δ*gng-1*::*gng-1*, and truncated complementation strain Δ*gng-1*::*gng-1*$_{1–85}$ were cultured on solid medium at 28°C for 20 h. Mutant Δ*gng-1* displayed phialides, marked with red arrowheads, whereas neither the parental strain Δ*ku70* nor the complementation strain Δ*gng-1*::*gng-1* did. Scale bar = 100 μm. (**B**) Magnified phialides are marked with red arrowheads. Scale bar = 25 μm. (**C**) Numbers of asexual spores produced by *P. oxalicum*. Fungal strains were cultured on plates containing Avicel or SCS for 7 days, glucose for 8 days, or PDA for 4 days. Each data point is a mean ± standard deviation. $^{**}P < 0.01$ indicates differences between the mutant Δ*gng-1* and parental strain Δ*ku70*, complementation strain Δ*gng-1*::*gng-1*, or Δ*gng-1*::*gng-1*$_{1–85}$ on Student's *t* test. PDA: potato dextrose agar; MMM: modified minimal medium; SCS: soluble corn starch

GNG-1 modulates the mRNA levels of major PBDE genes, known regulatory genes, fungal development-related genes, and sugar-transporter-encoding genes in *P. oxalicum*

RNA-Seq was used to investigate the genome-wide changes in mRNA expression that resulted from the deletion of the *gng-1* gene in *P. oxalicum*. After preculture in glucose for 24 h, strains Δ*gng-1* and Δ*ku70* were cultured in MMM containing Avicel for 24 h, and their total RNAs were extracted and sequenced. The transcriptomic data generated were reliable, with a Pearson's correlation coefficient of $R^2 > 0.96$ and a principal components analysis for three biological repetitions of each strain (Supplementary Fig. S3). A comparative

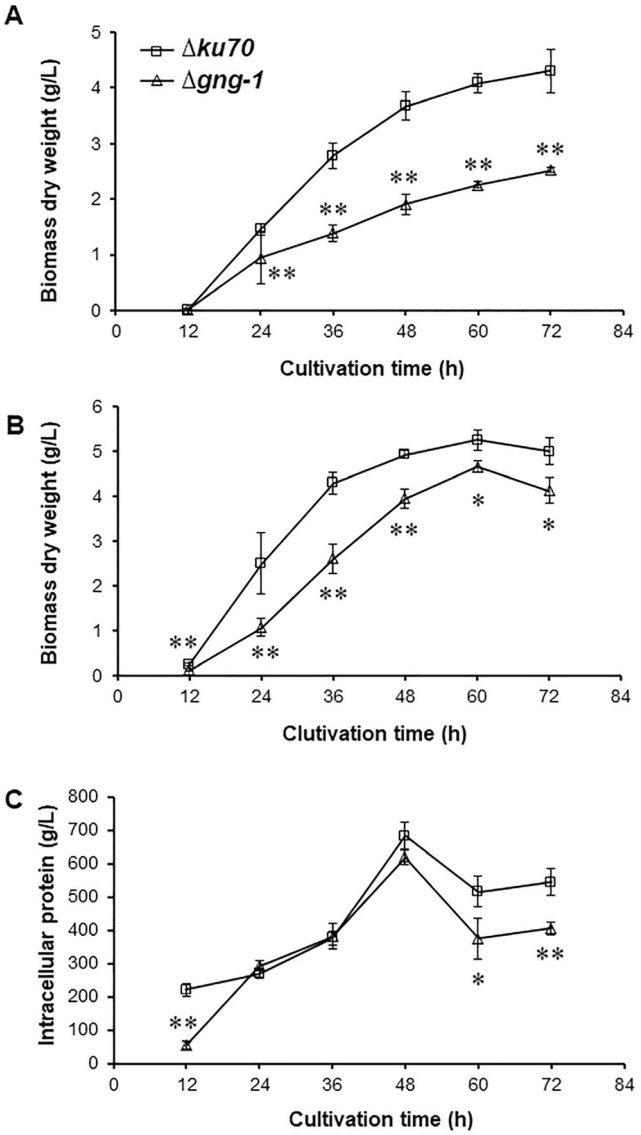

Fig. 5 Growth curves of *P. oxalicum* mutant Δ*gng-1* and parental strain Δ*ku70*. (**A**) Growth curves measured in MMM containing glucose; (**B**) growth curves measured in MMM containing SCS; (**C**) growth curves measured in MMM containing Avicel. The appropriate medium was directly inoculated with the asexual spores (1×10^8) of each *P. oxalicum* strain and incubated for 72 h at 28°C with shaking at 180 rpm. Data points represent means ± standard deviations. MMM: modified minimal medium; SCS: soluble corn starch

analysis of these transcriptomes identified 1329 differentially expressed genes (DEGs) (Supplementary Table S2), with thresholds of |log2(fold change)| ≥ 1.0 and $q \leq 0.05$. These consisted of 739 upregulated and 590 downregulated genes. Kyoto Encyclopedia of Genes and Genomes (KEGG) annotation showed that approximately 80% of the DEGs were involved in metabolism, specifically carbohydrate metabolism and amino acid metabolism (Fig. 6A).

Screening the 1329 DEGs identified 146 genes encoding putative CAZymes. The transcript levels of 63% of these genes reduced in Δ*gng-1*, with log2 (fold change) ranging from −5.5 to −1.0. Strikingly, among these 146 DEGs, 17 cellulase genes were detected, including cellobiohydrolase gene *POX05587/Cel7A-2*, endo-β-1,4-glucanase genes *POX05571/Cel7B* and *POX07535/Cel12A*, β-glucosidase gene *POX06835/Cel3A*, and six endo-β-1,4-xylanase genes, such as *POX00063/Xyn10A* and *POX06783/Xyn11A*. The transcripts levels of all these genes in Δ*gng-1* showed 50.8 to 97.8% reduced transcripts in the Δ*gng-1* compared with that in the parental strain Δ*ku70* (Fig. 6B).

Interestingly, three amylase genes (raw-starch-degrading glucoamylase gene *PoxGA15A* [*POX01356*] and α-glucosidase genes *POX03741* and *POX08147*) were also detected among the DEGs, and their transcript levels were reduced by 81.2%, 50.2%, and 73.0% in Δ*gng-1*, respectively (Fig. 6B).

It should be noted that the deletion of *gng-1* must have altered the expression of TF-encoding genes because TFs directly control gene expression. A total of 41 TF-encoding DEGs were identified, including 19 upregulated ($1.1 < \log_2$ [fold change] < 7.3) and 22 downregulated genes (−2.9 < log2 [fold change] < -1.0). Nine genes (*POX00972*, *POX02484*, *cxrB* [*POX04420*], *POX05145*, *POX05726*, *brlA* [*POX06534*], *flbD* [*POX07099*], *POX09124*, and *POX09469*) have previously been shown to regulate PBDE production to various extents (Yan et al. 2017; Zhao et al. 2016, 2019a, 2019b; Qin et al. 2013). Of these, the mRNA levels of three genes (*POX00972*, *POX02484*, and *cxrB*) were downregulated by 66.3–81.5% in Δ*gng-1* compared with their expression in Δ*ku70*, whereas the others were upregulated 2.2–85.7-fold in Δ*gng-1* (Fig. 6B). CxrB positively regulates cellulase and xylanase production (Yan et al. 2017). BrlA negatively controls cellulase production and positively regulates fungal conidiation (Qin et al. 2013). In addition to *brlA*, another two genes that are required for fungal conidiation, *abaA* (*POX07025*) and *flbD* (Ojeda-López et al. 2018), showed 16-fold increases in their transcript levels in Δ*gng-1*.

Sugar transporters are required for the expression of PBDE genes in filamentous fungi, specifically cellodextrin transporters (Li et al. 2013). Therefore, the effects of *gng-1* on the expression of genes encoding putative sugar transporters were investigated. We screened the 1329 DEGs annotated with the InterPro database using IPR005828 (major facilitator, sugar transporter-like), IPR005829 (sugar transporter, conserved site), and IPR003663 (sugar/inositol transporter). A total of 28 DEGs encoding putative sugar transporters were altered at the transcription level in Δ*gng-1*, with log2 (fold change) ranging from −2.7 to 6.6. Remarkably, the transcripts of the *POX05915* gene encoding the cellodextrin transporter CdtD were reduced by 54.3%, whereas the *POX07227* and *POX07576* genes, encoding the homologues of the glucose transporters RCO-3 (Madi et al. 1997) and GLT1 (Wang et al. 2017a, b) of *N. crassa*, respectively, were upregulated by 20.4- and 53.7-fold, respectively (Fig. 6B).

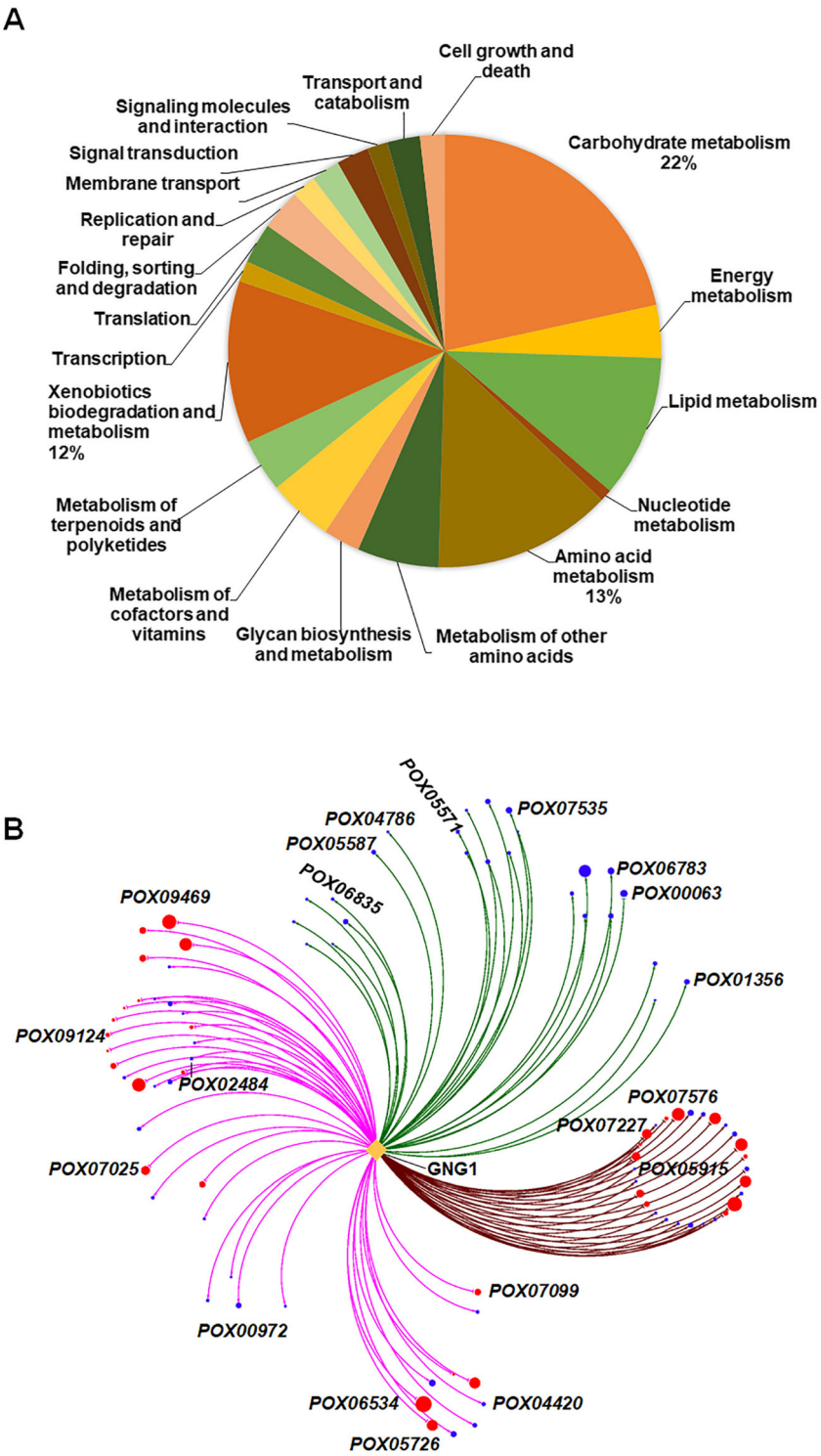

Fig. 6 Transcriptomic analysis of *P. oxalicum* mutant Δ*gng-1* and the parental strain Δ*ku70* grown in MMM containing Avicel as the sole carbon source. (**A**) Differentially expressed genes (DEGs) in Δ*gng-1* annotated with the KEGG database. DEGs were detected with thresholds of $|\log2(\text{fold change})| \geq 1$ and $q \leq 0.05$. (**B**) DEGs encoding PBDEs, putative transcription factors, and sugar transporters are shown with green, purple, and dark red lines, respectively. Red and blue circles indicate up- and downregulated DEGs in mutant Δ*gng-1*. Sizes of circles were calculated as 10 × log2 (fold change). MMM: modified minimal medium; KEGG: Kyoto Encyclopedia of Genes and Genomes

Strikingly, transcripts of the *POX00158* gene, which encodes a FUS3/FSS1-like MAP kinase, were reduced by 66.1% in the mutant Δ*gng-1* compared with their expression in Δ*ku70* (Supplementary Table S2).

To confirm the effects of *gng-1* on the expression of PBDE genes in *P. oxalicum*, reverse transcription (RT)-real-time quantitative PCR (RT-qPCR) was used. *P. oxalicum* strains Δ*gng-1* and Δ*ku70* were cultured for 4–48 h in MMM containing Avicel at 28°C with shaking at 180 rpm. The tested genes are shown in Fig. 7. The expression of all the tested genes was downregulated by 27.7–99.5% in the mutant Δ*gng-1* at 4–24 h of Avicel induction compared with their expression in Δ*ku70*. In contrast, at 48 h, the transcripts of *POX06783/Xyn11A* had decreased by 87.1%, whereas the

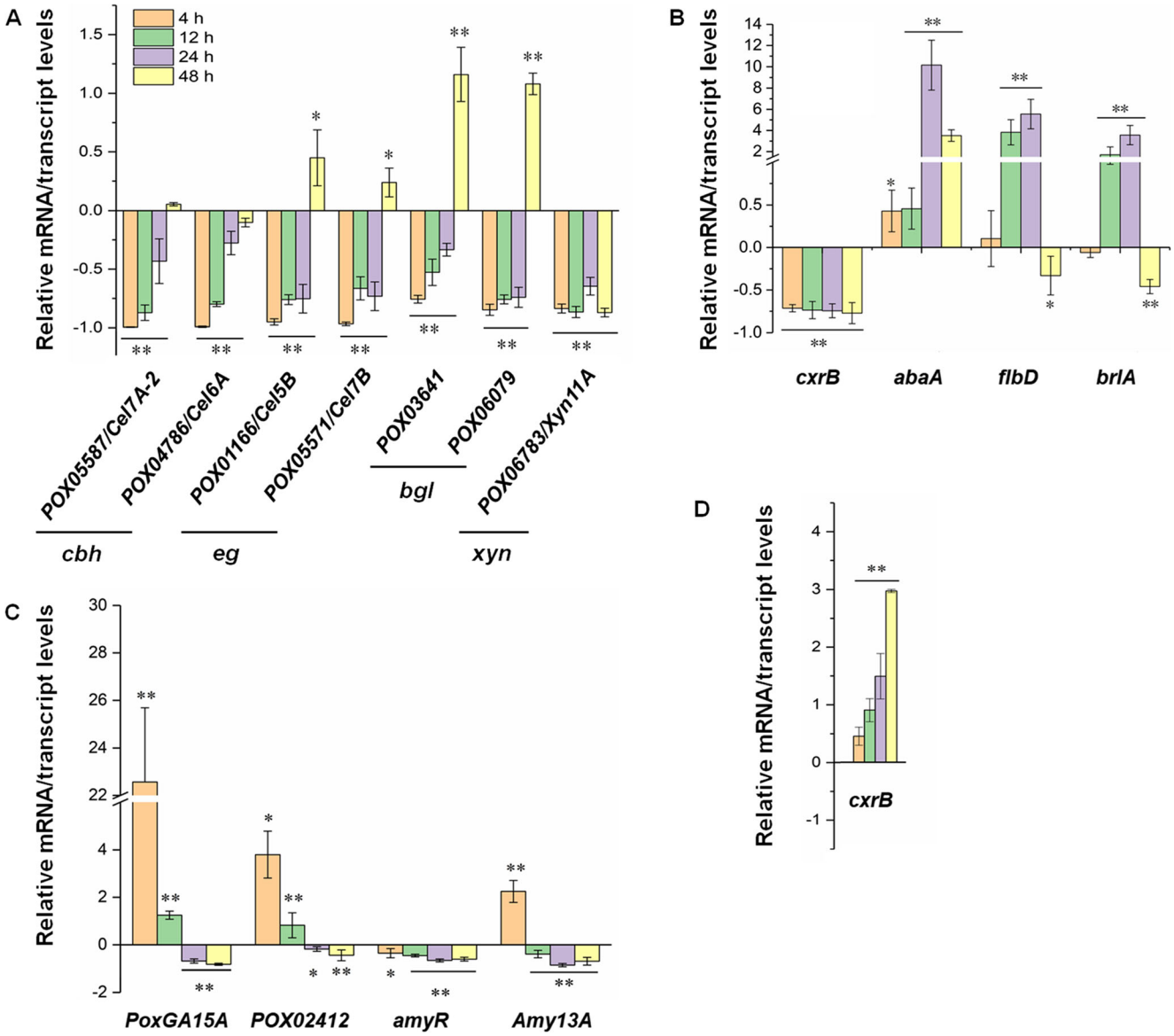

Fig. 7 Regulation of gene mRNA levels by GNG-1 in *P. oxalicum* detected with RT–qPCR. (**A**) The mRNA levels of key cellulase and xylanase genes in the mutant Δ*gng-1* cultured in the presence of Avicel for 4–48 h. *cbh*: cellobiohydrolase gene; eg: endo-β-1,4-glucanase gene; *bgl*: β-1,4-glucosidase gene; *xyn*: endo-xylanase gene. (**B**) mRNA levels of known regulatory genes in mutant Δ*gng-1* cultured in the presence of Avicel for 4–48 h. CxrB regulates the expression of cellulase and xylanase genes in *P. oxalicum*, whereas BrlA, AbaA, and FlbD are involved in asexual development. (**C**) mRNA levels of major amylase genes and their regulatory gene in mutant Δ*gng-1* cultured in the presence of soluble corn starch for 4–48 h. Raw-starch-degrading enzyme gene, *PoxGA15A*; glucoamylase gene, *POX02412*; α-amylase gene, *amy13A*; regulatory gene, *amyR*. (**D**) *cxrB* mRNA levels in Δ*gng-1*::*cxrB* cultured in the presence of Avicel for 4–48 h. Gene mRNA levels in mutant Δ*gng-1*::*cxrB* were normalized against the levels in the parental strain Δ*ku70*. Data points represent means ± standard deviations. $^{**}P \le 0.01$ and $^{*}P \le 0.05$ on Student's *t* test, indicating significant differences between the deletion mutant and the parental strain Δ*ku70*

transcript levels of *POX01166/Cel5B*, *POX05571/Cel7B*, *POX03641*, and *POX06079* had increased by 23.8–116.1% (Fig. 7A).

The transcript levels of four key regulatory genes, *cxrB*, *brlA*, *abaA*, and *flbD*, were also investigated in *P. oxalicum* with RT–qPCR assays. The transcripts of *cxrB* were downregulated in the mutant Δ*gng-1* during the whole period of culture, whereas the transcripts of *abaA* were upregulated. The transcripts of both *brlA* and *flbD* increased at 12–24 h but decreased again at 48 h (Fig. 7B).

Whether the expression of major amylase genes is affected by GNG-1 was analyzed with RT-qPCR. After preculture in glucose medium, *P. oxalicum* strains Δ*gng-1* and Δ*ku70* were cultured for 4–72 h in MMM containing SCS as the sole carbon source and their total RNA was extracted. The genes tested included *PoxGA15A*, *POX02412*, *Amy13A*

(*POX09352*), and their regulatory gene *amyR* (*POX03890*). The mRNA levels of all the tested amylase genes were 2.2–22.6-fold higher in Δ*gng-1* than in Δ*ku70* at 4 h after induction. The expression of *amyR* was reduced by 35.4%. At 12 h, the transcripts of *PoxGA15A* and *POX02412* had increased by 82.2% and 1.2-fold, respectively, in Δ*gng-1*, whereas those of *amyR* and *Amy13A* had decreased by 45.5% and 39.2%, respectively. After 12 h, the transcripts of all the tested genes decreased in Δ*gng-1* by 18%–85.7% (Fig. 7C).

The requirement of GNG-1 for PBDE production, but not for fungal conidiation, is replaced by constitutive overexpression of the regulatory gene *cxrB*

The known regulatory gene *cxrB* was among the DEGs controlled by *gng-1*. Therefore, we speculated that the involvement of *gng-1* in PBDE gene expression might depend on *cxrB*. To test this hypothesis, *cxrB* was constitutively overexpressed in the mutant Δ*gng-1*. The constructed strain Δ*gng-1*::*cxrB* was confirmed (Supplementary Fig. S1D) with PCR using specific primers (Supplementary Table S1). In Δ*gng-1*::*cxrB*, the transcription of *cxrB* increased by 45.5% to 3-fold after Avicel induction for 4–48 h compared with that in the Δ*ku70* (Fig. 7D). Interestingly, the production of all cellulases and xylanases by Δ*gng-1*::*cxrB* in the presence of Avicel, and the production of SSDEs and RSDEs on SCS, were restored to the levels in both the parental strain Δ*ku70* and the complementation strain Δ*gng-1*::*gng-1* ($P > 0.05$; Fig. 2).

The phenotypes of Δ*gng-1*::*cxrB* on plates containing glucose, SCS, or Avicel or on PDA plates were similar to those of Δ*ku70*, except with a slight change in colony color (Fig. 3). Strangely, Δ*gng-1*::*cxrB* displayed early conidiophore production compared with that in Δ*ku70* and Δ*gng-1::gng-1* after culture for 20 h on all the carbon sources tested (Avicel, starch, and glucose) and PDA plates, similar to that in mutant Δ*gng-1*. The mutant Δ*gng-1*::*cxrB* showed fewer hyphal branches than Δ*ku70* or Δ*gng-1::gng-1* but more than Δ*gng-1* (Fig. 4; Supplementary Fig. S2). Moreover, the numbers of asexual spores produced by mutant Δ*gng-1*::*cxrB* was restored to the level of spore production by Δ*ku70* (Fig. 4C). These results indicate that CxrB, acting downstream from GNG-1, and its overexpression (partially) compensated for the deletion of *gng-1* in PBDE production and fungal development.

CxrB positively regulates the production of RSDEs and SSDEs in *P. oxalicum*

GNG-1 affects amylase production of *P. oxalicum*, and constitutively expressed *cxrB* restored the amylase production of the mutant Δ*gng-1* to the level in the parental strain Δ*ku70*, suggesting that CxrB regulates the production of amylase in *P. oxalicum*. To confirm this, the mutant Δ*cxrB*, parental strain Δ*ku70*, and complementation strain Δ*cxrB*::*cxrB* (Yan et al. 2017) were cultured at 28°C for 2–4 days in MMM containing SCS as the sole carbon source. Both SSDE and RSDE production in mutant Δ*cxrB* reduced by 32.6%–53.5% compared with that in the parental strain Δ*ku70* ($P < 0.01$). The complementation strain Δ*cxrB*::*cxrB* secreted similar amounts of SSDEs and RSDEs to Δ*ku70* (Fig. 8A), verifying that CxrB regulated amylase production in *P. oxalicum*.

CxrB indirectly regulates the mRNA levels of major amylase genes by controlling the regulatory gene *amyR* and directly regulates the expression of fungal development-related genes

When the mutant Δ*cxrB* was cultured in MMM containing SCS as the sole carbon source, the transcription levels of major amylase genes, including *PoxGA15A*, *Amy13A*, *POX02412*, and *amyR*, was investigated with RT-qPCR. The parental strain Δ*ku70* was used as the control. At 4 h after induction, the mRNA levels of all the genes tested were upregulated by 92.0% to 7.3-fold in Δ*cxrB* compared with that in Δ*ku70*. At 12 h, the transcript levels of *PoxGA15A* and *amy13A* had increased by 180.1% and 70.1%, respectively, in Δ*cxrB*, whereas the other genes were downregulated by 50.8–51.8%. After induction for 12 h, all the tested genes in Δ*cxrB* were downregulated by 38.2–92.1%, except *Amy13A* at 24 h ($P < 0.05$; Fig. 8B).

An in vitro electrophoretic mobility shift assay (EMSA) was used to determine whether CxrB binds the promoter regions (500–1000 bp upstream) of major amylase genes and their regulatory gene *amyR*. A DNA fragment from gene *POX05989*, encoding β-tubulin, was used as the control. The putative DNA-binding domain at $CxrB_{194–302}$, which contains two C2H2-type zinc fingers, was recombinantly expressed in *Escherichia coli* and purified, fusing with thioredoxin (Trx)-, a histidine (His)- and S-tag (Yan et al. 2017; Supplementary Fig. S4). No delayed band was observed when the recombinant protein $rCxrB_{194–302}$ was tested with 6-FAM (fluorescein azide) -labeled probes from the three amylase genes, or the control proteins bovine serum albumin (BSA) and Trx–His–S, and DNA fragments competitive probes and control probe (Supplementary Fig. S5). Interestingly, delayed bands appeared when the *amyR* probe was added to 1.6–2.0 μg of $rCxrB_{194–302}$. Neither BSA nor Trx–His–S interacted with the *amyR* probe. The competitive *amyR* probe, without 6-FAM, considerably impeded the interaction between $rCxrB_{194–302}$ and the *amyR* probe (Fig. 9A). These data suggested that CxrB specifically bound the promoter region of *amyR*.

In addition to amylolytic genes, the effects of CxrB on the mRNA levels of the fungal development-related genes *brlA* and *flbD* were observed under Avicel induction. The expression of *brlA* and *flbD* in the mutant Δ*cxrB* increased by 40.3%

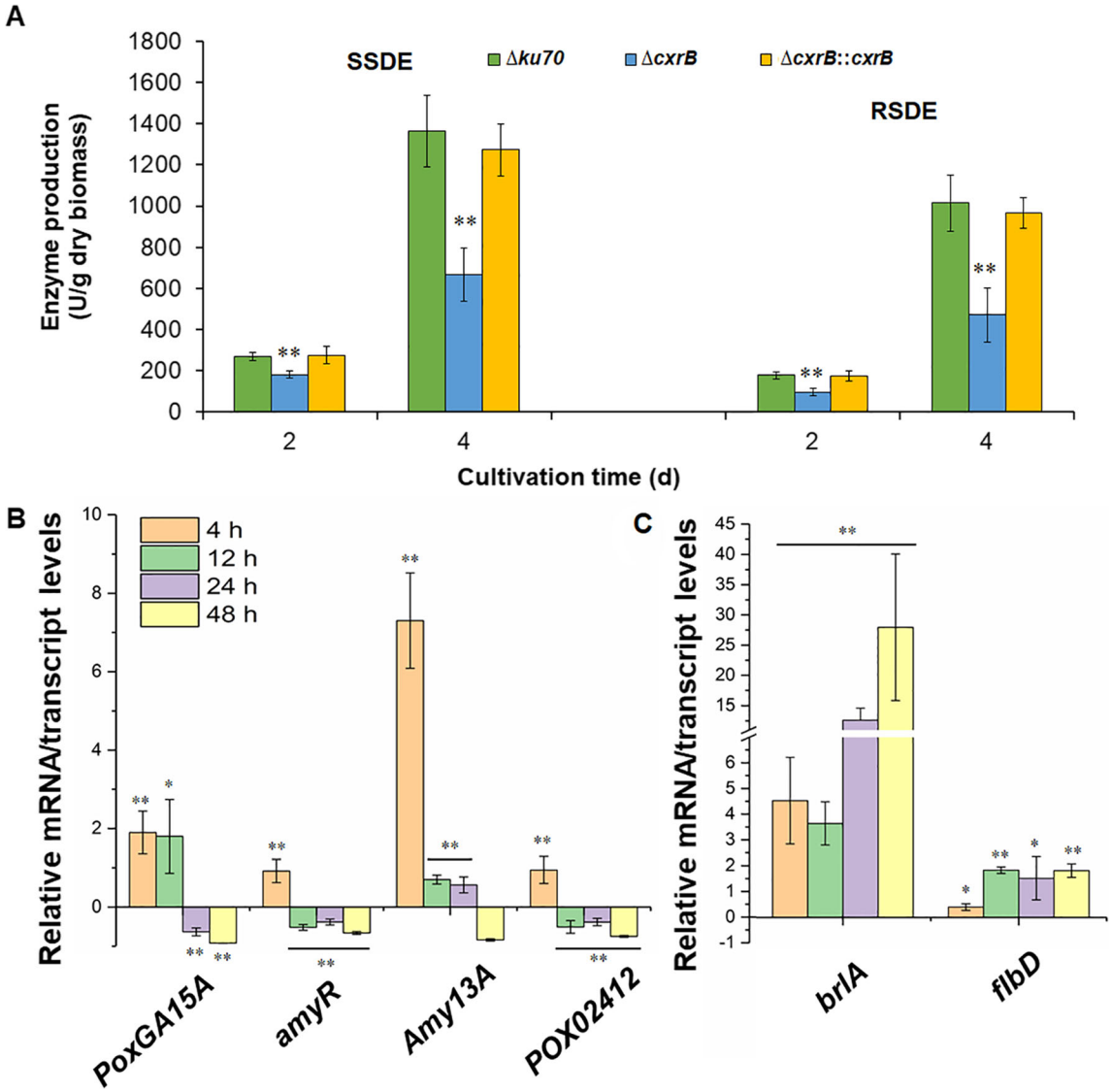

Fig. 8 Effects of CxrB on amylase production (**A**) and mRNA levels of essential amylase genes (**B**) and asexual-development-related genes (**C**) in *P. oxalic*um. After their transfer from glucose, fungal strains were cultured in MMM containing soluble corn starch for 2–4 days to test amylase production (**A**), for 4–48 h to test gene expression (**B**), or in MMM containing Avicel for 4–48 h (**C**) at 28°C with shaking at 180 rpm. Gene mRNA levels in mutant Δ*gng-1* were normalized against the levels in the parental strain Δ*ku70*. $^{**}P \leq 0.01$ and $^{*}P \leq 0.05$ by Student's *t*-test, indicate significant differences between the deletion mutant and the parental strain Δ*ku70*. MMM: modified minimal medium; SSDE: soluble-starch-degrading enzyme; RSDE: raw-cassava-starch-degrading enzyme. Data points represent means ± standard deviations

to 28-fold during the whole culture period compared with that in the parental strain Δ*ku70* ($P < 0.05$; Fig. 8C). In vitro EMSA and competitive EMSA also confirmed that recombinant $rCxrB_{194–302}$ specifically bound the promoter regions of *brlA* and *flbD* (Fig. 9B and C).

CxrB localizes in the nucleus

To visualize the subcellular localization of CxrB in *P. oxalicum*, recombinant strains carrying the green fluorescent protein (GFP)-labeled fusion protein CxrB–GFP were constructed with homologous recombination (Supplementary Fig. S6A). The expression of the fusion gene *cxrB–gfp* was controlled by the Avicel-induced promoter pPoxEGCel5B (Wang et al. 2018). The recombinant strains generated were confirmed with PCR (Supplementary Fig. S6B–F) using specific primers (Supplementary Table S1). When the various strains were cultured in MMM containing Avicel as the sole carbon source, the fluorescent GFP signals were predominantly detected in the cell nuclei and merged well with the fluorescence of 4′,6-diamidino-2-phenylindole (DAPI) (Fig. 10), which is used for the microscopic detection of nuclei and nuclear DNA in live cells (Tarnowski et al. 1991).

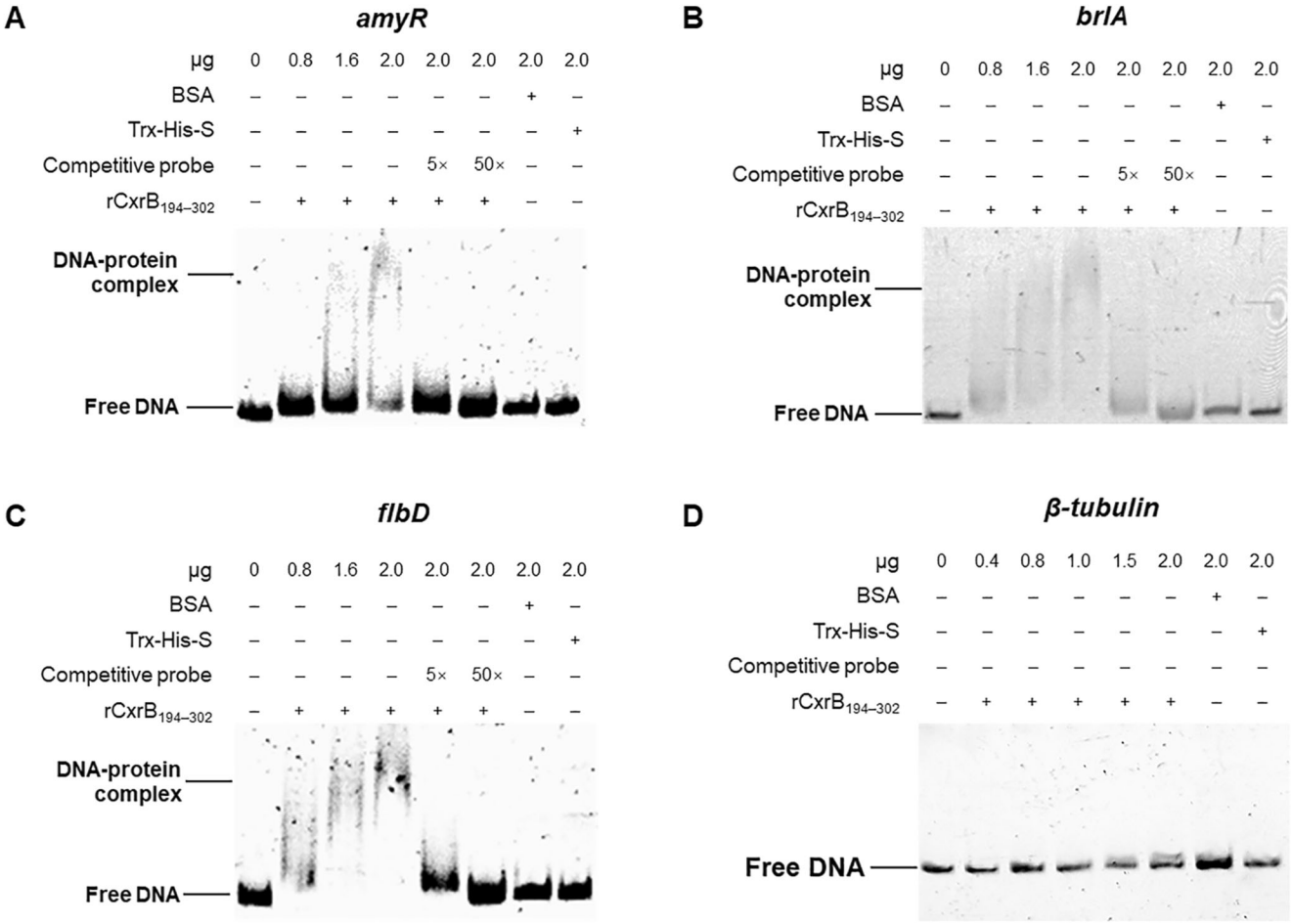

Fig. 9 Interaction between CxrB and target genes revealed by in vitro electrophoretic mobility shift assay (EMSA). (**A**) Regulatory gene *amyR*. (**B**) Regulatory gene *brlA*. (**C**) Regulatory gene *flbD*. Recombinant protein $rCxrB_{194–302}$ (0–2.0 μg) was mixed with 50 ng of FAM-labeled probes. In each EMSA reaction, nonspecific sheared salmon sperm DNA was added to prevent nonspecific binding between the protein and probes. Probes without the FAM label were used for the competitive EMSA. BSA, Trx–His–S fusion protein, or the promoter region of the β-tubulin gene alone were used as controls. FAM, 6-carboxyfluorescein; BSA, bovine serum albumin

Discussion

In this study, we characterized the roles of putative G protein γ subunit GNG-1 in *P. oxalicum* in detail. GNG-1 modulated PBDE (cellulase, xylanase and amylase) production in *P. oxalicum* under Avicel or SCS induction and the expression of major PBDE genes. Importantly, we have shown for the first time that GNG-1 affects the production of amylase and xylanase and the expression of major amylase and xylanase genes. GNG-1 modulates the expression of PBDE genes might through affecting the expression of regulatory gene *cxrB*. CxrB directly regulates the expression of major cellulase and xylanase genes on Avicel (Yan et al. 2017) and indirectly regulates the transcripts of major amylase genes through controlling the expression of another regulatory gene *amyR* under SCS induction in *P. oxalicum* (Fig. 11). AmyR is required for amylase production by directly regulating the major amylolytic genes, such as the α-amylase gene *amy13A* and the glucoamylase gene *amy15A*, in *P. oxalicum*, *Aspergillus* sp., and *Talaromyces pinophilus* under starch induction (Li et al. 2015; Zhang et al. 2017; Ma et al. 2021).

A question attacks our attention that how GNG-1 mediates the expression of *cxrB*. A possible mechanism is that GNG-1 activates downstream MAP kinase and cAMP-dependent signal cascades that modulate the expression of cellulase and xylanase genes (Schmoll 2018; Ma et al. 2021; Wang et al. 2017a, b). The Gβ could interact with a MAPK scaffold Ste5 that anchored MAPKKK Ste11, MPKK Ste7 and MAPK Fus3 together (Alvaro and Thorner 2016). Recently, MAP kinase PoxMK1 as a homolog of Fus3 positively controlled the expression of *cxrB* in *P. oxalicum* (Ma et al. 2021). However, the exact signal pathway of G protein on regulation of cellulase and xylanase under Avicel induction still needs to be further studied.

It should also be noted that the deletion of *gng-1* in *P. oxalicum* reduced cellulase production, whereas the deletion of its orthologue *gng-1* in *T. reesei* enhanced cellulase production (Tisch et al. 2011). In *T. reesei*, the Gβ and Gγ

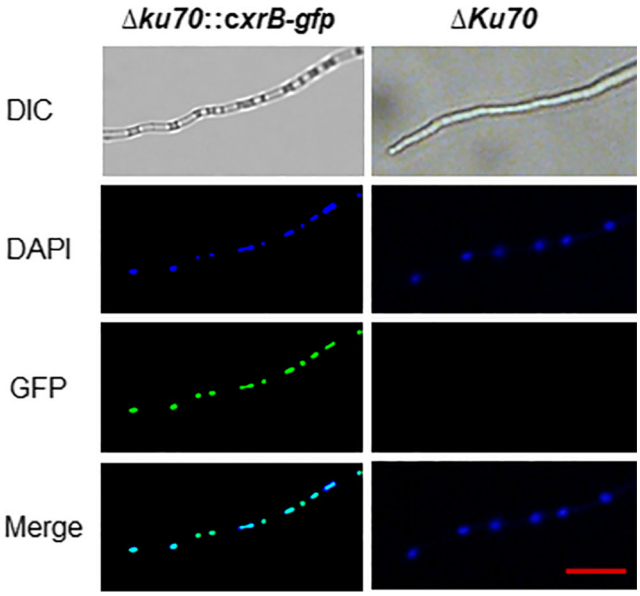

Fig. 10 Subcellular localization of CxrB in *P. oxalicum*. Transformants expressing CxrB–GFP were precultured in MMM with Avicel as the sole carbon source for 48 h at 28°C with a shaking at 180 rpm, and the parental strain Δ*ku70* was used as a control. The localization of CxrB was monitored by recording the GFP signal. Fungal nuclei were stained with 4',6-diamidino-2-phenylindole (DAPI). The samples were observed under a fluorescence microscope (Olympus DP480; Olympus, Tokyo, Japan). Scale bar = 25 μm

with their putative chaperone PhLP1 negatively influence the abundance of *rgs1* transcript, which leads to improved activity of the Gα GNA1. Deletion of *gna-1* abolishes the expression of major cellulase gene in light but enhances it in darkness. Surprisingly, constitutive activation of GNA1 only enhanced the expression of cellulase genes in the presence of both cellulose and light (Schmoll 2018). Surprisingly, mutant Δ*gng-1* of *T. reesei* reduced the transcriptional levels of major cellulase genes but increased cellulase secretion, which might be due to post-transcriptional regulation (Tisch et al. 2011). However, there are insufficient evidence supporting those conclusions thus far, and the detail studies must be carried out in future. Clearly, signal transduction and regulation of cellulase gene expression in *T. reseei* are different from that in *P. oxalicum*.

Moreover, the C-terminal CCAAX motif contributed to the production of cellulase, hyphal conidiospores, and asexual spores, but not to hyphal branching in *P. oxalicum*. When Gβγ is released from the activated heterotrimeric G protein, it activates the downstream MAP kinase cascade, which occurs at the plasma membrane because Gβγ is firmly tethered there by the CCAAX motif in Gγ, with the aforementioned lipophilic moieties (Alvaro and Thorner 2016). The lack of the CCAAX motif affects the anchoring of Gβγ to the plasma membrane, altering the downstream signal transduction pathways. The mutant Δ*gng-1::gng-1*$_{1–85}$ retained approximately 70% of the cellulase production of its parental strain Δ*ku70*, implying that an alternative pathway activated by Gγ or an Gγ-independent pathway is also involved in the regulation of cellulase gene expression in *P. oxalicum*. Strangely, the C-terminal CCAAX motif did not contribute to xylanase production, which may be attributable to the balance of the regulatory network formed by downstream TFs. It should be noted that these results may also be attributable to the different levels of mRNA and protein expressed from an alternative locus (*POX05007*) or the involvement of the cAMP pathway, which is modulated by Gα, but these possibilities require further study.

In addition to PBDE production, GNG-1 was also required for the vegetative growth and conidiation of *P. oxalicum* and the expression of related genes, such as *brlA* and *flbD*, as has been reported in *A. nidulans*, *T. reesei*, and *N. crassa* (Tisch et al. 2011; Krystofova and Borkovich 2005; Seo et al. 2005).

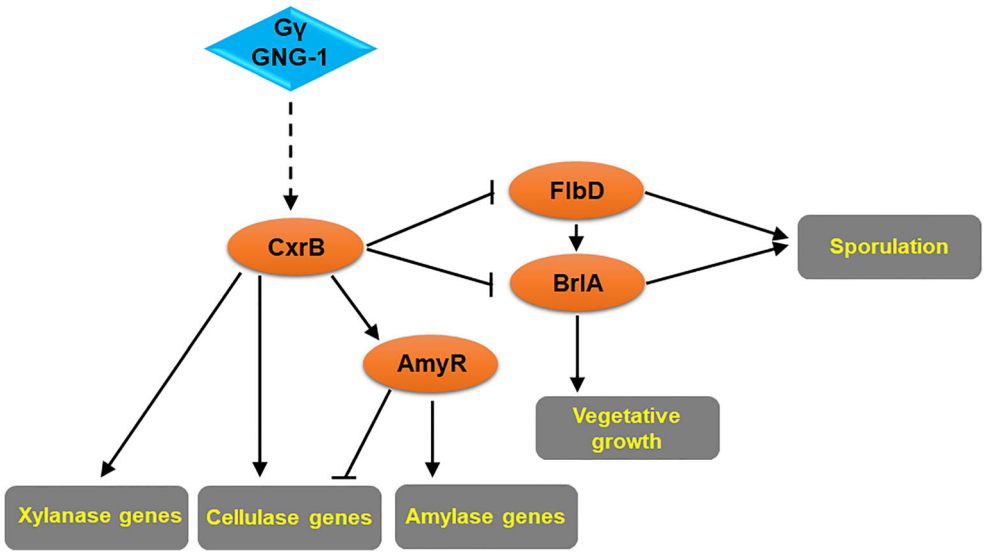

Fig. 11 Schematic model of the proposed roles of G protein gamma subunit GNG-1 modulated by the downstream transcription factor CxrB in *P. oxalicum*. Dashed line indicates that how GNG-1 modulates the expression of *cxrB* is unknown. Bold lines with arrows represent activation and barred lines represent inhibition

Importantly, in this study, we have also shown that CxrB directly bound the promoter regions of both *brlA* and *flbD* to repressed their expression under Avicel induction (Fig. 11). BrlA and FlbD are essential for asexual sporulation in filamentous fungi, and FlbD activates the expression of *brlA* (Qin et al. 2013; Arratia-Quijada et al. 2012). The deletion of either *cxrB* or *brlA* affects the vegetative growth of *P. oxalicum* (Yan et al. 2017; Qin et al. 2013). Although the early conidiation in Δ*gng-1* may result from the increased expression of *brlA* and *flbD*, the number of asexual spores produced by Δ*gng-1* significantly reduced, which might be attributable to the reduced mycelial biomass of Δ*gng-1*. The overexpression of *cxrB* in the mutant Δ*gng-1* partly restored hyphal branching, but did not restore conidiation to the level in Δ*ku70*, thus leading to spore production similar to that in Δ*ku70*. Other possible mechanisms still require investigation.

In summary, we found that GNG-1 modulated the expression of PBDE genes and mycelial-development-related genes, which depends on the implementation of the downstream transcription factor CxrB, and in this way, positively affected PBDE production and fungal development. The generated results extended the diversity of Gγ protein functions and provided new insight into the signal transduction and regulation of PBDE gene expression in filamentous fungi.

Supplementary Information The online version contains supplementary material available at https://doi.org/10.1007/s00253-021-11370-3.

Acknowledgements We thank Core Facility Center, specifically Mass Spectrometry Technology Platform from State Key Laboratory for Conservation and Utilization of Subtropical Agro-bioresources, Guangxi University, for technological support.

This work was financially supported by the grants from the National Natural Science Foundation of China (grants 31760023 and 31660305) to JXF and SZ, the Autonomous Research Project of State Key Laboratory for Conservation and Utilization of Subtropical Agro-bioresources (SKLCUSA-a201902 and SKLCUSA-a201923) to JXF, Training Program for 1000 Young and Middle-aged Key Teachers in Guangxi at 2019, and the One Hundred Person Project of Guangxi to SZ.

Author contribution SZ designed, supervised this study, and revised the manuscript. XMP performed mutant construction and measurement of enzymatic production, analysis of gene expressional levels and manuscript preparation. DT, TZ, and LSL were involved in mutant construction and data discussion. CXL carried out bioinformatic analyses. XML was involved in preparation of experimental materials. JXF was involved in data analysis and revised manuscript. All authors read and approved the final version of the manuscript.

Data availability All data generated or analyzed during this study are included in this published article.

Declarations

This article does not contain any studies with human participants or animals performed by any of the authors.

Conflict of interest The authors declare no competing interests.

References

Alvaro CG, Thorner J (2016) Heterotrimeric-G-protein-coupled receptor signaling in yeast mating pheromone response. J Biol Chem 291: 7788–7795

Arratia-Quijada J, Sánchez O, Scazzocchio C, Aguirre J (2012) FlbD, a Myb transcription factor of *Aspergillus nidulans*, is uniquely involved in both asexual and sexual differentiation. Eukaryot Cell 11:1132–1142

Benocci T, Aguilar-Pontes MV, Zhou M, Seiboth B, de Vries RP (2017) Regulators of plant biomass degradation in ascomycetous fungi. Biotechnol Biofuels 10:152

Chakravorty D, Assmann SM (2018) G protein subunit phosphorylation as a regulatory mechanism in heterotrimeric G protein signaling in mammals, yeast, and plants. Biochem J 475:3331–3357

Chen YX, Chen YS, Shi CM, Huang ZB, Zhang Y, Li SK, Li Y, Ye J, Yu C, Li Z, Zhang XQ, Wang J, Yang HM, Fang L, Chen Q (2018) SOAPnuke. a MapReduce acceleration-supported software for integrated quality control and preprocessing of high-throughput sequencing data. Gigascience 7:1–6

Gougoulias C, Clark JM, Shaw LJ (2014) The role of soil microbes in the global carbon cycle: tracking the below-ground microbial processing of plant-derived carbon for manipulating carbon dynamics in agricultural systems. J Sci Food Agric 94:2362–2371

Hu YB, Liu GD, Li ZH, Qin YQ, Qu YB, Song X (2013) G protein-cAMP signaling pathway mediated by PGA3 plays different roles in regulating the expressions of amylases and cellulases in *Penicillium decumbens*. Fungal Genet Biol 58–59:62–70

Kim D, Langmead B, Salzberg SL (2015) HISAT: a fast spliced aligner with low memory requirements. Nat Methods 12:357–360

Krystofova S, Borkovich KA (2005) The heterotrimeric G-protein subunits GNG-1 and GNB-1 form a Gβγ dimer required for normal female fertility, asexual development, and Ga protein levels in *Neurospora crassa*. Eukaryot Cell 4:365–378

Kumar S, Stecher G, Li M, Knyaz C, Tamura K (2018) MEGA X: molecular evolutionary genetics analysis across computing platforms. Mol Biol Evol 35:1547–1549

Langmead B, Salzberg SL (2012) Fast gapped-read alignment with Bowtie 2. Nat Methods 9:357–359

Li B, Dewey CN (2011) RSEM: accurate transcript quantification from RNA-Seq data with or without a reference genome. BMC Bioinformatics 12:323

Li LD, Wright SJ, Krystofova S, Park G, Borkovich K (2007) Heterotrimeric G protein signaling in filamentous fungi. Annu Rev Microbiol 61:423–452

Li J, Liu GD, Chen M, Li ZH, Qin YQ, Qu YB (2013) Cellodextrin transporters play important roles in cellulase induction in the cellulolytic fungus *Penicillium oxalicum*. Appl Microbiol Biotechnol 97: 10479–10488

Li ZH, Yao GS, Wu RM, Gao LW, Kan QB, Liu M, Yang P, Liu GD, Qin YQ, Song X, Zhong YH, Fang X, Qu YB (2015) Synergistic and dose-controlled regulation of cellulase gene expression in *Penicillium oxalicum*. PLoS Genet 11(9):e1005509

Li ZH, Liu GD, Qu YB (2017) Improvement of cellulolytic enzyme production and performance by rational designing expression regulatory network and enzyme system composition. Bioresour Technol 245:1718–1726

Li CX, Zhao S, Luo XM, Feng JX (2020) Weighted gene co-expression network analysis identifies critical genes for the production of cellulase and xylanase in *Penicillium oxalicum*. Front Microbiol 11: 520

Liu YH, Yang KL, Qin QP, Lin GN, Hu TR, Xu ZL, Wang S (2018) G protein α subunit GpaB is required for asexual development, aflatoxin biosynthesis and pathogenicity by regulating cAMP signaling in *Aspergillus flavus*. Toxins 10:117

Livak KJ, Schmittgen TD (2001) Analysis of relative gene expression data using real-time quantitative PCR and the $2^{-\Delta\Delta C}$T method. Methods 25(4):402–408

Love MI, Huber W, Anders S (2014) Moderated estimation of fold change and dispersion for RNA-seq data with DESeq2. Genome Biol 15:550

Ma B, Ning YN, Li CX, Tian D, Guo H, Pang XM, Luo XM, Zhao S, Feng JX (2021) A mitogen-activated protein kinase PoxMK1 mediates regulation of the production of plant-biomass-degrading enzymes, vegetative growth, and pigment biosynthesis in *Penicillium oxalicum*. Appl Microbiol Biotechnol 105:661–678

Madi L, McBride SA, Bailey LA, Ebbole DJ (1997) *rco-3*, a gene involved in glucose transport and conidiation in *Neurospora crassa*. Genetics 146:499

Ojeda-López M, Chen W, Eagle CE, Gutiérrez G, Jia WL, Swilaiman SS, Huang Z, Park HS, Yu JH, Cánovas D, Dyer PS (2018) Evolution of asexual and sexual reproduction in the aspergilli. Stud Mycol 91:37–59

Powers-fletcher MV, Kendall BA, Griffin AT, Hanson KE (2016) Filamentous fungi. Microbiol Spectr 4(3):DMIH2-0002-2015

Qin YQ, Bao LF, Gao MR, Chen M, Lei YF, Liu GD, Qu YB (2013) *Penicillium decumbens* BrlA extensively regulates secondary metabolism and functionally associates with the expression of cellulase genes. Appl Microbiol Biotechnol 97:10453–10467

Schmoll M (2018) Regulation of plant cell wall degradation by light in *Trichoderma*. Fungal Biol Biotechnol 5:10

Schmoll M, Schuster A, Silva RN, Kubicek CP (2009) The G-alpha protein GNA3 of *Hypocrea jecorina* (anamorph *Trichoderma reesei*) regulates cellulase gene expression in the presence of light. Eukaryot Cell 8(3):410–420

Schuster A, Tisch D, Seidl-Seiboth V, Kubicek CP, Schmoll M (2012) Roles of protein kinase A and adenylate cyclase in light-modulated cellulase regulation in *Trichoderma reesei*. Appl Environ Microbiol 78:2168–2178

Seibel C, Gremel G, Silva RN, Schuster A, Kubicek CP, Schmoll M (2009) Light-dependent roles of the G-protein alpha subunit GNA1 of *Hypocrea jecorina* (anamorph *Trichoderma reesei*). BMC Biol 7:58

Seo JA, Han KH, Yu JH (2005) Multiple roles of a heterotrimeric G-protein γ-subunit in governing growth and development of *Aspergillus nidulans*. Genetics 171:81–89

Tarnowski BI, Spinale FG, Nicholson JH (1991) DAPI as a useful stain for nuclear quantitation. Biotech Histochem 66(6):297–302

Tisch D, Kubicek CP, Schmoll M (2011) The phosducin-like protein PhLP1 impacts regulation of glycoside hydrolases and light response in *Trichoderma reesei*. BMC Genomics 12:613

Wang P, Nuss DL (1995) Induction of a *Cryphonectria parasitica* cellobiohydrolase I gene is suppressed by hypovirus infection and regulated by a GTP-binding-protein-linked signaling pathway involved in fungal pathogenesis. Proc Natl Acad Sci U S A 92: 11529–11533

Wang B, Li J, Gao J, Cai P, Han X, Tian C (2017a) Identification and characterization of the glucose dual-affinity transport system in *Neurospora crassa*: pleiotropic roles in nutrient transport, signaling, and carbon catabolite repression. Biotechnol Biofuels 10:17

Wang MY, Zhang ML, Li L, Dong YM, Jiang Y, Liu KM, Zhang RQ, Jiang BJ, Niu KL, Fang X (2017b) Role of *Trichoderma reesei* mitogen-activated protein kinases (MAPKs) in cellulase formation. Biotechnol Biofuels 10:99

Wang L, Zhao S, Chen XX, Deng QP, Li CX, Feng JX (2018) Secretory overproduction of a raw starch-degrading glucoamylase in *Penicillium oxalicum* using strong promoter and signal peptide. Appl Microbiol Biotechnol 102(21):9291–9301

Yan YS, Zhao S, Liao LS, He QP, Xiong YR, Wang L, Li CX, Feng JX (2017) Transcriptomic profiling and genetic analyses reveal novel key regulators of cellulase and xylanase gene expression in *Penicillium oxalicum*. Biotechnol Biofuels 10:279

Zhang Z, Liu JL, Lan JY, Duan CJ, Ma QS, Feng JX (2014) Predominance of *Trichoderma* and *Penicillium* in cellulolytic aerobic filamentous fungi from subtropical and tropical forests in China, and their use in finding highly efficient beta-glucosidase. Biotechnol Biofuels 7:107

Zhang T, Zhao S, Liao LS, Li CX, Liao GY, Feng JX (2017) Deletion of *TpKu70* facilitates gene targeting in *Talaromyces pinophilus* and identification of *TpAmyR* involvement in amylase production. World J Microbiol Biotechnol 33:171

Zhao S, Yan YS, He QP, Yang L, Yin X, Li CX, Mao LC, Liao LS, Huang JQ, Xie SB, Nong QD, Zhang Z, Jiang L, Xiong YR, Duan CJ, Liu JL, Feng JX (2016) Comparative genomic, transcriptomic and secretomic profiling of *Penicillium oxalicum* HP7-1 and its cellulase and xylanase hyper-producing mutant EU2106, and identification of two novel regulatory genes of cellulase and xylanase gene expression. Biotechnol Biofuels 9:203

Zhao S, Liao XZ, Wang JX, Ning YN, Li CX, Liao LS, Liu Q, Jiang Q, Gu LS, Fu LH, Yan YS, Xiong YR, He QP, Su LH, Duan CJ, Luo XM, Feng JX (2019a) Transcription factor Atf1 regulates expression of cellulase and xylanase genes during solid-sate fermentation of ascomycetes. Appl Environ Microbiol 85:e01226–e01219

Zhao S, Liu Q, Wang JX, Liao XZ, Guo H, Li CX, Zhang FF, Liao LS, Luo XM, Feng JX (2019b) Differential transcriptomic profiling of filamentous fungus during solid-state and submerged fermentation and identification of an essential regulatory gene PoxMBF1 that directly regulated cellulase and xylanase gene expression. Biotechnol Biofuels 12:103